



Journal of Applied and Computational Mechanics



Research Paper

Mechanical Characterisation and Comparison of Hyperelastic Adhesives: Modelling and Experimental Validation

Francisco J. Simon Portillo¹, Óscar Cuadrado Sempere², Eduardo A.S. Marques³,
Miguel Sánchez Lozano⁴, Lucas F.M. da Silva⁵

¹ Department of Mechanical and Energy Engineering, Universidad Miguel Hernández, Elche, 03202, Spain, Email: f.simon@umh.es

² Department of Mechanical and Energy Engineering, Universidad Miguel Hernández, Elche, 03202, Spain, Email: ocuadrado@umh.es

³ Department of Mechanical and Energy Engineering, Universidad Miguel Hernández, Elche, 03202, Spain, Email: msanchez@umh.es

⁴ Institute of Science and Innovation in Mechanical and Industrial Engineering (INEGI), Porto, 4200-465, Portugal, Email: emarques@inegi.up.pt

⁵ Department of Mechanical Engineering, Faculty of Engineering, University of Porto, Porto, 4200-465, Portugal, Email: lucas@fe.up.pt

Received September 07 2021; Revised November 04 2021; Accepted for publication November 20 2021.

Corresponding author: M. Sánchez Lozano (msanchez@umh.es)

© 2022 Published by Shahid Chamran University of Ahvaz

Abstract. This work focuses on the mechanical characterisation of adhesives with hyperelastic behaviour, and on the determination of the behavioural laws that best represent them, in order to be able to introduce them into simulation models. There are virtually no references to the characterisation of these materials in the literature, so it has been decided to use the methodologies commonly employed with other hyperelastic materials, such as rubber, whose behaviour is similar to that of highly flexible adhesives. Firstly, a test plan is carried out on simple specimens, uniaxial and planar configurations, designed to measure the non-linear behaviour of the adhesives in both tension and shear. Subsequently, using finite element models of the tested specimens, different behavioural laws from those usually used for the representation of hyperelastic materials are tested. Based on the experimental results, the parameters of the different laws proposed are adjusted, and the results are compared. In conclusion, it has been determined that the Mooney-Rivlin model is the one that allows the best fit, and therefore may be the most suitable to represent the behaviour of hyperelastic adhesives. For the adhesive used in this work, the obtained law has been validated by comparing the results of tests on single lap adhesive joint (SLJ) specimens with the results predicted by the simulation.

Keywords: Flexible adhesive, Hyperelastic models, Mechanical characterisation, Finite element analysis.

1. Introduction

In recent years, the use of composite materials has become widespread in a wide range of applications, with a particularly marked increase in the aerospace and automotive industries. This is due to the excellent stiffness-to-weight and strength-to-weight ratios of these materials. Highly flexible structural adhesives in particular are increasingly being used in engineering [1]. They are predominantly used where considerable expansion and contraction are expected at the joint, in the case of materials with different coefficients of thermal expansion (CTE), in joints between different metals, fibre-reinforced plastics, or glass panels, or where a highly flexible bond is required [2]. Hyperelastic adhesives also offer good sealing properties when tolerances and gaps are high. They also have advantages such as the ability to withstand impact, high vibration, and safety, which are critical values in the automotive industry. Finally, a safety advantage of hyperelastic adhesives over rigid adhesives is that they prevent sudden failure, as they have a high resistance to tear propagation, allowing damaged joints to be identified and repaired before complete rupture.

The adhesives used in this research behave in a similar way to rubber and other elastomers, they show elastic behaviour in the large deformation range, showing a non-linear relationship between load and deformation [3], but maintaining their capacity for a total recovery of the deformation when the stress ceases. It is for this reason that its modelling as a hyperelastic material is proposed, which we will see in detail in the following sections.

The extended area of use of these adhesives requires an extensive and detailed testing methodology to certify the behaviour and reliability of the joints. Different appropriate methodologies have been proposed to experimentally analyse the hyperelastic behaviour of flexible adhesives [4-7]. However, there are very few studies dedicated to the analytical modelling of flexible bonds [8-9]. Almost all existing bond models have been developed for rigid adhesives [10].



The Finite Element Method (FEM) is currently the usual calculation procedure in structural mechanics and solid mechanics in general. The aim is always to reduce the time required for the project or for placing the product on the market. When this tool was not available, it was necessary to manufacture prototypes, test them and make improvements iteratively, which entailed a high cost, both financially and in terms of development time. Most of the analyses carried out are still based on the solution of static linear problems, where the value of the load does not vary as a function of time and there is a linear relationship between force and deformation (Hooke's Law) [11], which require the determination of few properties to characterise the behaviour of the material. Nevertheless, there is a growing development of numerical tools that allow an accurate prediction of the different behaviours and failure scenarios that can occur in complex composite materials. However, the modelling of non-linear or time- and strain rate-dependent behaviour, which is now possible thanks to the advance of these calculation capabilities, requires a much more complex characterisation, using the most appropriate techniques for each material. This is the case for flexible adhesives, which tend to have a viscous hyperelastic behaviour, which, in many cases, has not been sufficiently studied.

The first objective of this research is to analyse the behaviour and performance of different hyperelastic adhesives currently used on the industrial level, using the manufacture and testing of Halterio and Single Lap Shear (SLJ) specimens [7]. Based on the results obtained in the tests, the adhesive with the best performance is selected, and its hyperelastic behaviour is characterised, to subsequently undertake its numerical modelling. For this modelling, different hyperelastic constitutive models were first studied, which a priori could be valid to reproduce the mechanical behaviour of the flexible adhesive. Characterisation tests have been carried out on different specimens, subjected to uniaxial tension and pure shear, using specific test geometries taken from standards and previous works [12-13]. From the data of these tests and with the help of finite element programmes, the parameters of the different hyperelastic models have been adjusted, finally selecting those with which a better adjustment has been achieved by simulation of the stress-strain relationships extracted in the tests. Once the hyperelastic model has been adjusted, it should be possible to use it to simulate the behaviour of different joint configurations. To corroborate this, and to validate the selected material model, SLJ joints with different adhesive thicknesses have been computationally modelled, comparing the results with those obtained experimentally by testing specimens with the same configurations.

2. Hyperelastic Models and Methodology for Adjustment and Selection

The behaviour of hyperelastic materials is usually characterised using the strain energy density function [14]. This function acts as a potential of the stresses, unlike an elastic material, where there is a function that can directly relate the stresses to the strains in a linear fashion.

Elastic:

$$\sigma = F(\epsilon) \quad (1)$$

Hyperelastic:

$$\sigma = \frac{\partial W}{\partial \epsilon} \quad (2)$$

where ϵ is a dimensional strain of a solid and W (sometimes written as U) is the strain energy density or stored energy function defined per unit volume.

In order to characterise the mechanical behaviour of materials with hyperelastic behaviour, many theoretical models have been developed (Mooney-Rivlin, Ogden, Yeoh, etc.), obtained from the study of simple geometries and stresses (uniaxial compression, uniaxial tension, shear, etc.) [15].

The implementation of such models would be very complex without the help of finite element programmes, which have become a fundamental tool to determine in each case the most appropriate material model to reproduce the behaviour, and to help in the identification of the parameters. Among the large number of models proposed, this work focuses on those most commonly implemented by commercial finite element programs.

2.1 Common hyperelastic models

There is a considerable amount of literature on the modelling of materials with hyperelastic behaviour. The choice of model depends on the application, the relevant variables, and the data available to determine the material parameters. In order to achieve good results, the validity of the possible models should be studied, and the simplest model that can provide sufficient accuracy should be selected.

An efficient hyperelastic model can be explained by four main qualities [16]:

- It must be able to reproduce the full S-shaped response of the rubber exactly.
- The change of deformation modes should not be problematic, i.e. if the model works in uniaxial tension, it should also be accurate in shear or equibiaxial tension.
- The number of fit material parameters should be small, in order to reduce the number of experimental tests for their determination.
- The mathematical formulation must be simple so that the numerical performance of the model is feasible.

Rivlin proposed [17], that the strain energy density function (W) could be expressed as a polynomial of:

The main elongations

$$W = W(\lambda_1, \lambda_2, \lambda_3) \quad (3)$$

Deformation invariants

$$W = W(I_1, I_2, I_3) \quad (4)$$

where:



$$\lambda = \frac{L}{L_0} \quad (5)$$

where λ is principal elongation (the ratio of the length of the deformed element (L) to the initial length (L_0) for each of the principal directions)[18].

Deformation invariants:

$$I_1 = (\lambda_1)^2 + (\lambda_2)^2 + (\lambda_3)^2 \quad (6)$$

$$I_2 = (\lambda_1 \cdot \lambda_2)^2 + (\lambda_2 \cdot \lambda_3)^2 + (\lambda_3 \cdot \lambda_1)^2 \quad (7)$$

$$I_3 = (\lambda_1 \cdot \lambda_2 \cdot \lambda_3)^2 \quad (8)$$

For incompressible materials [19]: $I_3 = 1$.

If the material can be assumed to be incompressible, as is often the case with rubbers, the volumetric terms are neglected. However, this requires that the Poisson's ratio is close to 0.5 at low stresses, which is the property of the adhesives used in this research.

Starting from the proposition made by Rivlin, the deformation energy density function shown below was arrived at [17]:

$$W = \sum_{i+j=1}^N c_{ij} \cdot (I_1 - 3)^i \cdot (I_2 - 3)^j + \sum_{i=1}^N \frac{1}{D_i} \cdot (J^c - 1 - R)^{2i} \quad (9)$$

where:

W : Strain energy density function.

N : A positive determining the number of terms in the strain energy function ($N = 1,2,3$).

c_{ij} : Are empirically determined material constants.

I_1, I_2 : First and second deformation invariants.

J : Elastic volume ratio.

D_i : Coefficient defining the compressibility of the material.

R : Coefficient defining the volumetric expansion with temperature change.

The Rivlin expression given above is somewhat complex to apply, and successive researchers have developed particular cases of this expression, which have subsequently been implemented in the various finite element programmes.

Two types of models of hyperelastic materials are available in the Abaqus programme (one of the most widely used in this field of application) and each model defines the strain energy function in a different way [20-21]. One is phenomenological models that treat the problem from the perspective of continuum mechanics and characterise the stress-strain behaviour without reference to the microscopic structure. Another is physically motivated models that consider the material response from the perspective of microstructure. A brief review of the phenomenological hyperelastic models available in Abaqus, and used during this study, is given below.

Mooney-Rivlin model

It is a phenomenological model based on the deformation invariants and has as its general expression [22]:

$$W = \sum_{i+j=1}^N c_{ij} \cdot (I_1 - 3)^i \cdot (I_2 - 3)^j \quad (10)$$

Other models have been derived from this model, such as Neo-Hookean, James-Green-Simpson, Signorini, Yeoh, Peng, Peng-Landel.

Neo-Hookean model

This model is a special case of the Mooney-Rivlin form with $c_{01} = 0$ and can be used when material data is insufficient. It is easy to use and can make a good approximation at relatively small deformations.

$$W = c_{10}(I_1 - 3) \quad (11)$$

where c_{10} is a material constant and I_1 first deformation invariant.

Polynomial model

This strain energy function model is commonly used in modelling the stress-strain behaviour of elastomers, with four or five terms. The polynomial model represented in equation is in the compressible form, based on the invariants $I_1 - I_2$ of the Cauchy-Green deviatoric tensor [14], making W become:

$$W = \sum_{i=1}^N c_{ij} \cdot (I_1 - 3)^i \cdot (I_2 - 3)^j + \sum_{i=1}^N \frac{1}{D_i} \cdot (J_{el} - 3)^{2i} \quad (13)$$

J_{el} : Elastic volume Ratio.

I_1, I_2 : First and second deformation invariant.



c_{ij} : Describes the shearing behaviour of the material.

D_i : Determines compressibility, zero for totally incompressible materials.

N : Determines the number of terms in the strain energy function ($N = 1,2,3$).

Yeoh model

Yeoh [23] developed a new phenomenological model based on cubic invariants and proposed the following form as the deformation energy density equation:

$$W = c_{10}(I_1 - 3) + c_{20}(I_1 - 3)^2 + c_{30}(I_1 - 3)^3 \quad (13)$$

where c_{10} , c_{20} and c_{30} are material constant and I_1 first deformation invariant.

This model has the characteristic that the shear modulus varies with deformation and only depends on the first deformation invariant. Yeoh established the cubic equation to predict the stress-strain behaviour in different deformation modes, but especially in parts with high shear influence such as a tyre.

Ogden model

It is a model [24] based on the principal deformations, its general expression being:

$$W = \sum_{n=1}^N \frac{\mu_n}{\alpha_n} \cdot (\lambda_1^{\alpha_n} + \lambda_2^{\alpha_n} + \lambda_3^{\alpha_n} - 3) \quad (14)$$

where α_n and μ_n are empirically determined material constants and the second term represents volumetric changes.

These models make the following assumptions: the material behaviour is elastic, the material behaviour is isotropic, the material is incompressible, the simulation will include non-linear geometrical effects[25].

Research carried out by various authors yields the following conclusions [16]:

- The Ogden model requires more computational time as it is an exponential function.
- The determination of the values of the Mooney-Rivlin constants from experimental tests is easier than the Ogden constants.
- The potential strain energy equation of the Mooney-Rivlin model is considered the most widely used constitutive law in the stress analysis of elastomers.

2.2 Model fitting based on tests

Equation (9) shows the typical equation for hyperelastic models according to which the behaviour is determined, on the one hand by the principal invariants, and, on the other hand, by the volumetric properties. The deviatoric properties are determined from experimental test data under various stress states. To define the input requirements of the models, several tests are required. Before defining the types of tests that will allow the most accurate model fitting, different sources of information have been consulted. On many occasions, these were publications related to the characterisation of rubbers [26], as we have already mentioned, the adhesives used in this research behave in a similar way to rubber. The manuals of the finite element programmes normally suggest that the most accurate way to determine the hyperelastic coefficients is to estimate them from a combination of two or three of the following tests: uniaxial tension, planar tension and equibiaxial tension tests. In this study, we decided to use the combination of the planar and uniaxial test for the adjustment.

Uniaxial stress

A very common experiment on materials with hyperelastic behaviour. The most important requirement is that the length of the sample must be greater than the width and thickness. The aim is to create an experiment where there are no lateral restrictions for sample thinning [26].

Principal deformations:

$$\lambda_1 = \frac{L}{L_0}; \lambda_2 = \lambda_3 = \frac{1}{\sqrt{\lambda}} \quad (15)$$

where λ_j ($j = 1,2,3$) is the principal stretch ratio. Also A and L , respectively, mean the cross-sectional area and length of a specimen.

Principal stresses:

$$\sigma_1 = \sigma = \frac{P}{A_0}; \sigma_3 = \sigma_2 = 0 \quad (16)$$

where P is the load and σ_j ($j = 1,2,3$) is the axial stress.

The most common specimen geometry for this type of test and material with hyperelastic behaviour is the shape of a dumbbell or dog bone, defined in the standard ISO 37:2005 [27] (Fig. 1).

In this study, adhesive sheets of dimensions 200 x 130 with a thickness of 3 mm were created to produce the specimens. After 7 days of curing, dog bone shaped specimens were made from the sheet with suitable punching tools.

As very low forces were expected, due to the cross-section of the specimen and the low adhesive strength compared to other materials, a load cell with 1000 N full scale was used, using a universal testing machine (Fig. 2), with a test speed of 500 mm/min. Strain data were extracted using the DIC technique, according to the standard.



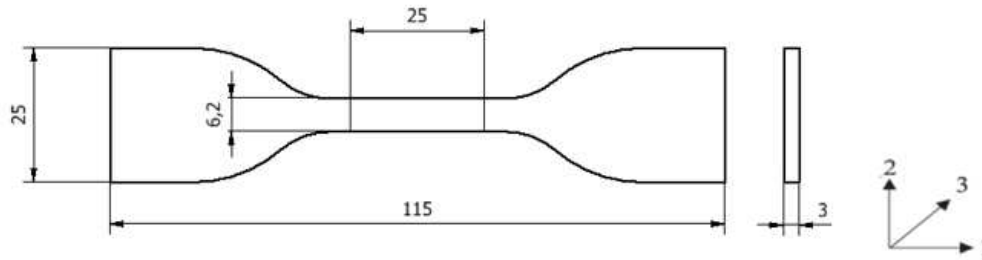


Fig. 1. Uniaxial tension specimen.

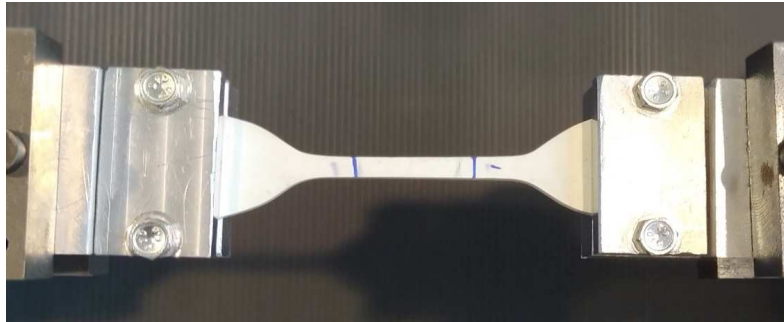


Fig. 2. Uniaxial tensile test.

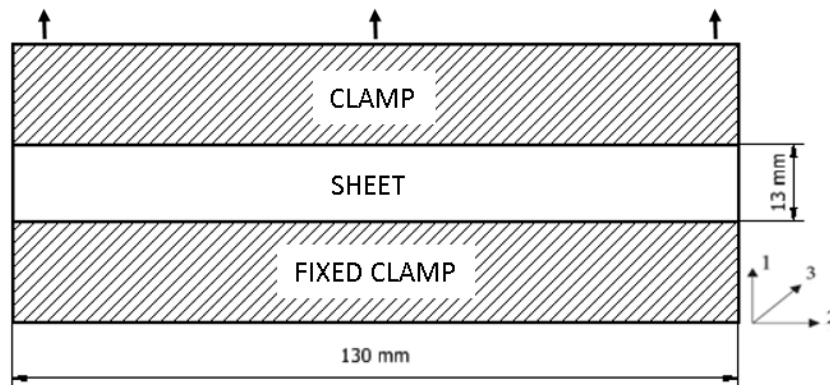


Fig. 3. Planar specimen.

Planar tension

The pure shear test is applied on several occasions to characterise the stress-strain, strength and fatigue properties of soft materials. It consists of a thin rectangular sheet that is clamped along its long edges to prevent lateral shrinkage (in direction 2) while stretched in the direction of its short edges (direction 1). The sheet can shrink freely in its thickness dimension (direction 3), to achieve homogeneity, and the width of the specimen should be greater than the height. The test piece is shown schematically in Fig. 2, and some examples can be found in the literature [25], [28]. The important feature of the pure shear test is that, unlike the uniaxial test described above (dog bone), no lateral deformations are induced, providing pure shear.

The states of deformation and stress are determined as follows:

Principal deformations:

$$\lambda_1 = \lambda; \lambda_2 = 1; \lambda_3 = \frac{1}{\lambda} \quad (17)$$

Principal stresses:

$$\sigma_1 = \sigma; \sigma_2 = 0; \sigma_3 = 0 \quad (18)$$

The dimensions of the effective tested area of the specimen in the planar test were 130 x 13 x 3 mm (Fig. 3). The specimens were obtained by cutting a previously cured sheet, in the same way as the dog bone specimens. In this case, the experiments were carried out at a deformation rate of 100 mm/min. Deformation data were also extracted using DIC [29], in addition to being able to detect possible debonding, or slippage, at the adhesive-metal interfaces (Fig. 4).



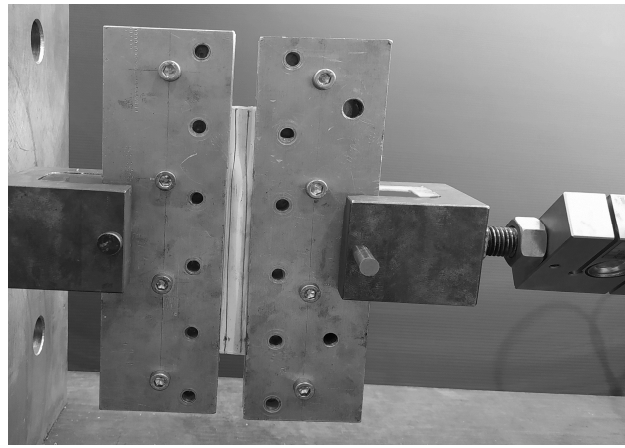


Fig. 4. Machine mounted planar tensile test.

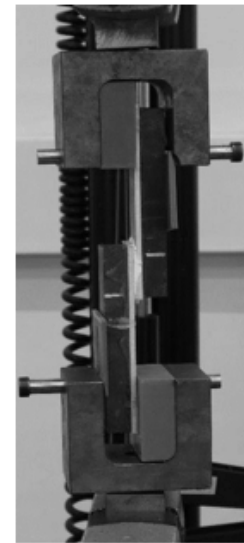
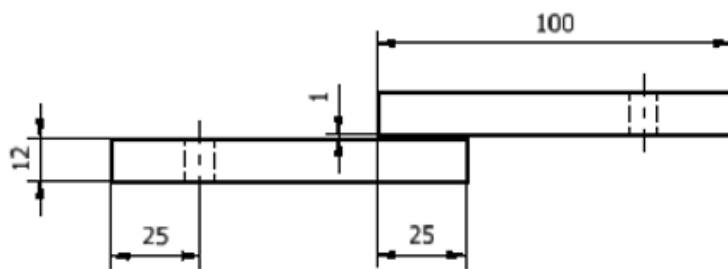


Fig. 5. SLJ specimen geometry (dimensions in mm).

2.3 Fitting of the material models. Estimation of hyperelastic constants

For the comparison between the different applicable models, and the estimation of the corresponding hyperelastic constants, the adjustment utility for these materials offered by the Abaqus software has been used. This material curve fitting utility allows the user to compare different hyperelastic material models, using data from uniaxial and planar tests. The input data to the programme are the nominal stress-nominal strain curves, from which the programme estimates the constants of the different possible models.

Of the various hyperelastic material models available, which can reproduce material behaviour at various levels of complexity, the material models initially considered were: Mooney-Rivlin, Neo-Hookean, Ogden ($N = 1$ and $N = 2$), Polynomial ($N = 2$). It should be noted that, in this case, the compressibility constants D_{ij} are zero for any of the models, as it is assumed to be an incompressible material.

The stress-strain curves obtained from simulation using each model are compared with the experimental ones. And the best fitting models are selected.

2.4 Validation and material model selection

The models of the hyperelastic material obtained, and the set of parameters adjusted experimentally with the help of Abaqus, have to be validated. To this end, it is proposed to test their performance in the simulation of standardised joint configurations. The simulation of tests of SLJ specimens with adhesive thicknesses of 1 and 3 mm is considered, comparing these with the experimental results obtained in the specimen tests using the same configuration and boundary conditions, as shown in Fig. 5. In this way, the best fitting model can be finally selected and, if necessary, fine tuning of the hyperelastic constants can be considered.

Despite recent developments, shear testing of materials using SLJ specimens is still the most widely used method, due to the performance and simplicity of fabrication. For the fabrication of these specimens, two key points must be taken into account: the alignment of the substrates and the control of the uniform thickness over the entire overlap surface. In order to carry out and guarantee a correct fabrication of these specimens, the use of forming tools is used. The most common standards describing the method are: ASTM D1002[30] and ISO 9664 [31]. In this research, it is intended that only shear stresses are produced, which are distributed evenly along with the adhesive layer. To achieve this, the joints have been manufactured in steel with dimensions of 100 x 25 x 10 mm, with an overlap length of 25 mm and adhesive thickness of 1 mm, as shown in Fig.5. With this geometry and material, no uncontrolled deformations occur in the adhesives during the test, avoiding the appearance of unwanted peeling stress components in the adhesive.



For the quasi-static simulation, as well as in the previous section, the commercial finite element software Abaqus has again been used. Quadratic hexahedral elements with reduced integration were used, in order to reduce the mesh density without affecting the accuracy of the solution (Fig. 6). A mesh convergence study was performed, comparing the results obtained with progressively finer mesh densities in the bonding area, until no significant differences were found in the final results using a higher mesh density than the one selected.

The force-displacement response was analysed up to a displacement range of 6 mm for the 1 mm thick specimen, and up to 12 mm for the 3 mm thick specimen. Non-linearities due to material law and large displacements were taken into account, but considering only the moments prior to the onset of failure. As fracture is not studied at this stage of the work, mesh refinement in the stress concentration zones was not considered necessary. For the non-linear calculation, the displacement range was divided into 900 steps. The convergence tolerances of the solver for the residuals were maintained at the default values offered by Abaqus, calculated respectively as 0.5% of the average forces and 1% of the displacement increment.

3. Experimental Development and Results

3.1 Adhesive selection

Four adhesives from different manufacturers are available, from which the one with the best performance will be selected to develop the following phases of this research work. The desired performance of these adhesives, in joints applied in the automotive field, is as follows:

- High elasticity.
- Low viscosity, thus avoiding heating of the adhesive in cyclic loading situations.
- Cohesive failure

The adhesives considered for the first part of this research are three one-component polyurethanes (PUR): SikaFlex 252, Korapur 140 and Bostik PU 2639 and another one based on silane-modified polymers (SMP) Teroson MS 939 (manufactured by Henkel), all designed to manufacture highly flexible seals. These products cure on reaction with moisture, forming high-performance elastomers. Depending on the adhesive, and according to the manufacturer's specifications, an adhesion promoter, in most cases, primer, is applied as part of the formulation.

To assess each adhesive with respect to these three points, two types of tests were performed: dog bone shaped specimens, based on ISO 37:2005[21] (Fig. 2), and SLJ joints (Fig. 5). The results are shown in Table 1 and Fig. 7.

In this first part of the research, 5 samples of each adhesive were tested using an Instron universal testing machine. The tests were carried out at constant speed, controlling the displacement at a rate of 5 mm/min for the SLJ specimen and 500 mm/min for the dog bone specimen.

Different types of failure (cohesive and adhesive) were observed, depending on the adhesive. The joints made with Bostick PU 2639 and Teroson MS 939 adhesive showed adhesive failure. Both have been discarded for this reason for the subsequent fitting of the hyperelastic model, as the model could not be validated until the elastic limit of the material was reached, due to the fact that the adhesive failure was reached earlier. Furthermore, it should be noted that Bostick PU 2639 adhesive has a high viscosity, which is also why it could not be considered a suitable material for cyclic loading resistance.

On the contrary, both SikaFlex 252 and Korapur 140 adhesive showed the desired type of cohesive bonding failure. Although Korapur 140 adhesive has a higher breaking strength, it has a significantly higher stiffness than SikaFlex 252. For this reason, SikaFlex 252 adhesive was finally selected for the next phases of the study, as the elasticity of the material is a key point in the selection of the adhesive, as mentioned above.

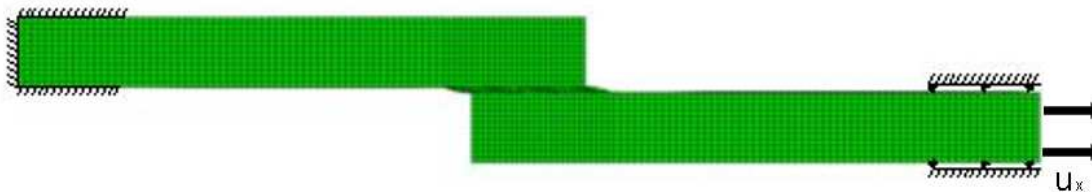


Fig. 6. FE simulation of SLJ specimen using Abaqus.

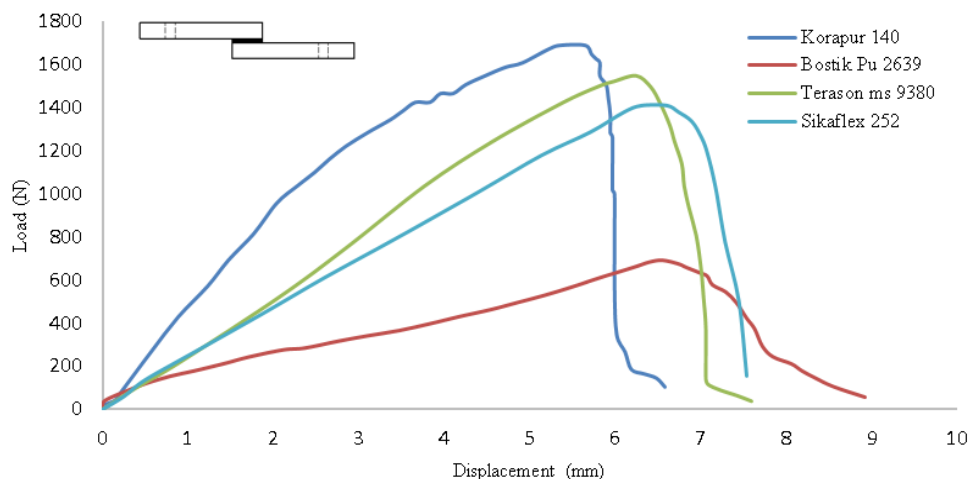


Fig. 7. Experimental result from SLJ tests using different adhesives.



Table 1. Mechanical properties obtained for different adhesives.

| Adhesive | Tensile strength (ISO 37) MPa | Shear strength (SLJ) MPa | Elongation at tear (ISO 37)% | 100 % Young module (ISO 37) MPa |
|----------------|-------------------------------|--------------------------|------------------------------|---------------------------------|
| Sika Flex 252 | 3.13 (±0.23) | 2.46(±0.3) | 480(±47.96) | 1.17(±0.047) |
| Korapur 140 | 3.18(±0.08) | 2.7(±0.09) | 381(±23.29) | 1.81(±0.02) |
| Bostik Pu 2639 | 1.07(±0.03) | 1.06(±0.12) | 975(±27.1) | 0.4(±0.01) |
| Terason ms 939 | 2.36(±0.23) | 2.42(±0.24) | 350(±8.6) | 1.22(±0.13) |

3.2 Model definition and estimation of hyperelastic constants

Figs. 8 and 9 show the stress-strain curves obtained respectively in the uniaxial tensile and planar tests, and compare them with those obtained for the same tests using the different material models automatically adjusted by the programme. The aim is to find a hyperelastic model that gives a good correlation between model and test for both types of test simultaneously.

Analysing the curves obtained in the low deformation zone, several of the models considered could be considered as a good option for predicting the experimental behaviour of the adhesive, both in the uniaxial tension and the planar test. On the other hand, for large deformations, a large dispersion is observed between the results obtained with the different models. The models with the best acceptable correlation over the whole deformation range are the following:

- The material model that appears to offer the most balanced fit for both test types, and over the entire strain range, is the Ogden model of order 2.
- The proposed Mooney-Rivlin model shows a much better correlation with the uniaxial tensile test results in the large strain range. Nevertheless, it shows an excessively high stiffness in the planar test simulation.

These material models will be the ones selected a priori to validate, in the following section, their behaviour in shear.

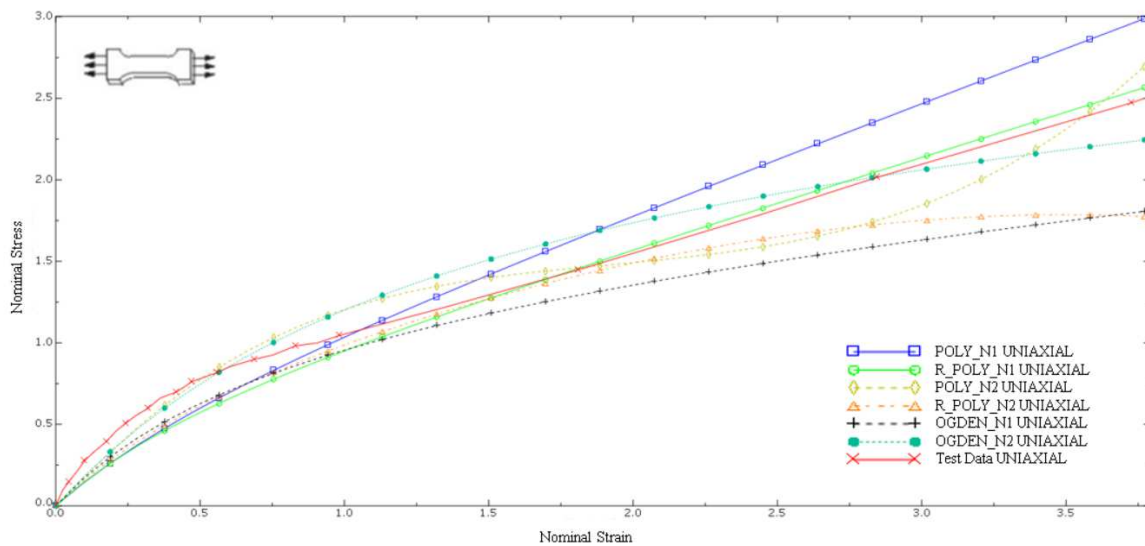


Fig. 8. Uniaxial test curves obtained for SikaFlex 252, using different behaviour laws.

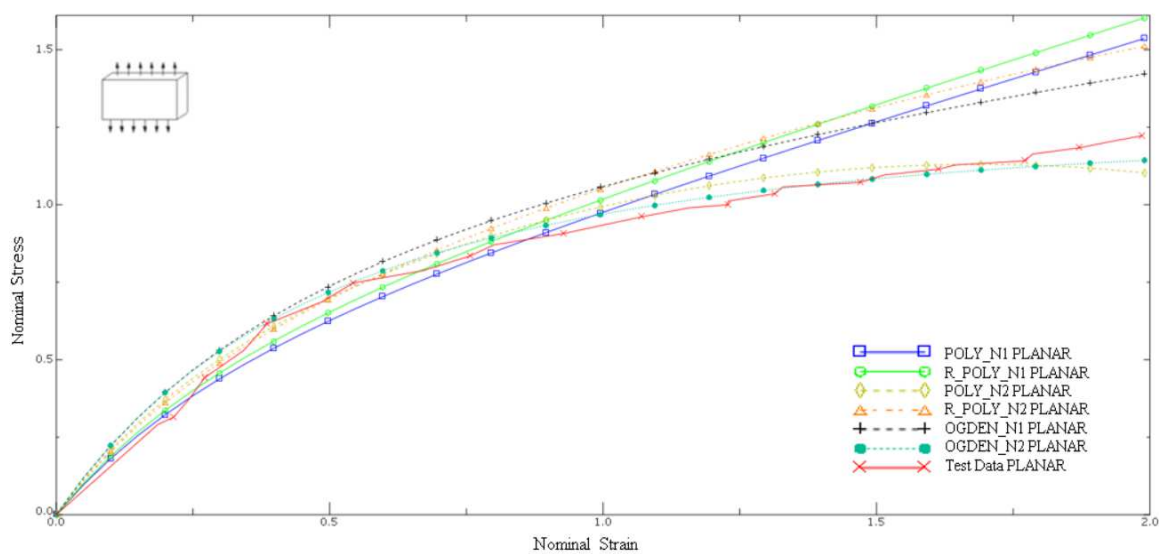


Fig. 9. Planar test curves obtained for SikaFlex 252, using different behaviour laws.



3.3 Validation through SLJ tests and final model selection

Next, the validation of the models of the a priori selected hyperelastic materials is addressed, following the methodology detailed in section 2.

Firstly, the Ogden $N=2$ model is used, with the adjusted constants shown in Table 2. Fig. 10 shows an acceptable correlation of results between simulation and test for the case of the specimen with 3 mm thick adhesive. But the model does not give good results in the simulation of the SLJ specimen with 1 mm thick adhesive (Fig. 11). Better results are obtained for the 1 mm thick when simulating the Ogden $N=1$ model, with the parameters adjusted for it in the previous section and shown in Table 3. However, the results obtained for the 3 mm thickness are vastly different from the experimental ones.

In view of these results, the objective of selecting and fitting a single hyperelastic model capable of reproducing the behaviour of end-joints with different configurations and thicknesses with acceptable accuracy, could not be considered to have been achieved. On the contrary, the results obtained with the Ogden model of orders 1 and 2 would corroborate the opinions of several authors regarding the need to perform characterisation tests with the same thickness of adhesive to be used in the final joints, as the only way to obtain a reliable adjustment of the material model, whose validity is thus restricted to the simulation of a very narrow range of possible joints.

An attempt was then made to validate the Mooney-Rivlin model fitted in the previous section, which offered a good correlation only in the simulation of the uniaxial tensile test. The first results showed that the model offered curves with shapes close to the experimental ones for both adhesive thicknesses, although not sufficiently accurate. After a slight iterative modification, the Mooney-Rivlin constants were set to the values shown in Table 4, with which a very good correlation was finally obtained for both SLJ tests, as shown in Figs. 10 and 11.

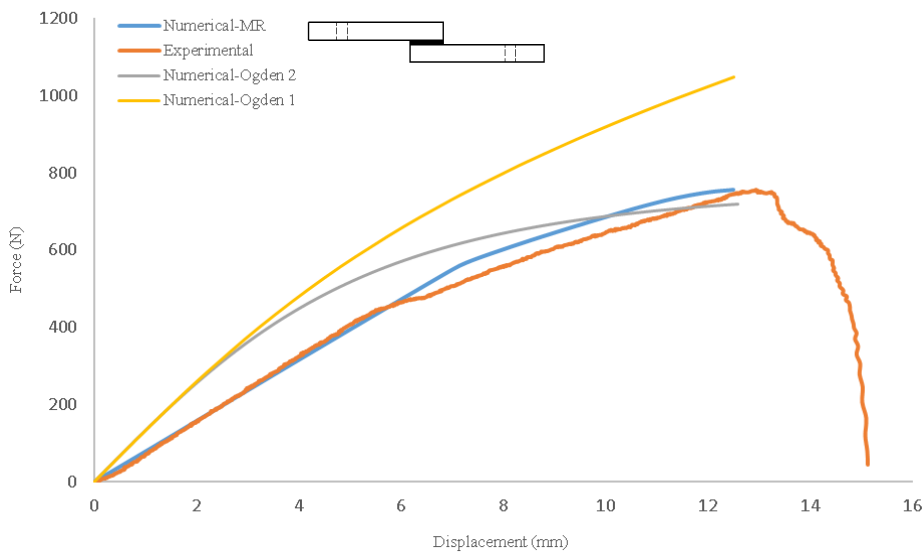


Fig. 10. Experimental and computational results for SLJ-3 mm of SikaFlex 252. Comparison between Ogden $N=2$, Ogden $N=1$ and Mooney Rivlin models.

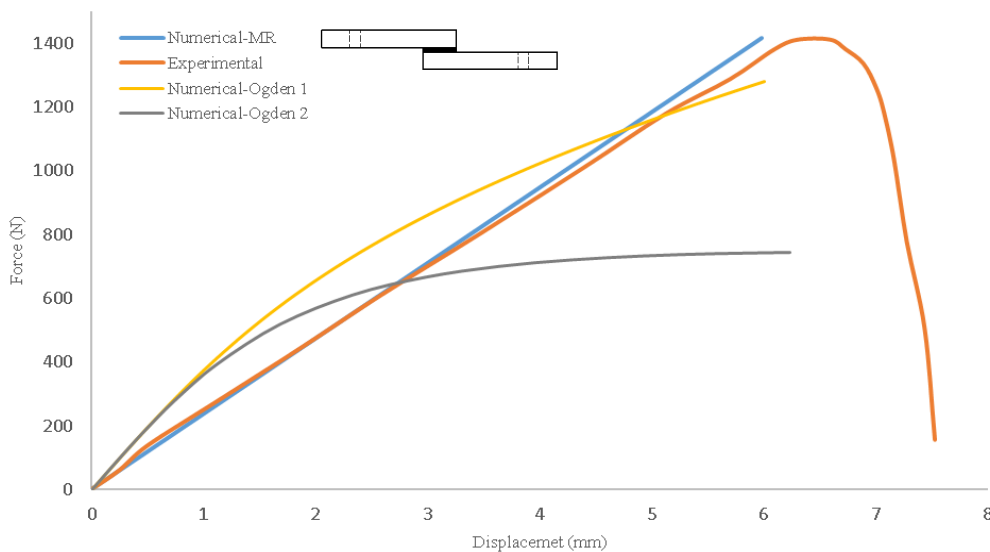


Fig. 11. Experimental and computational results for SLJ-1 mm of SikaFlex 252. Comparison between Ogden $N=2$, Ogden $N=1$ and Mooney Rivlin models.



Table 2. Ogden $N=2$ hyperelastic constants for SikaFlex 252.

| N | μ | α | D_1 |
|-----|--------------|-------------|-------|
| 1 | 1.32493862 | 1.19452984 | 0 |
| 2 | -0.677801657 | -1.35713429 | 0 |

Table 3. Ogden $N=1$ hyperelastic constants for SikaFlex 252.

| N | μ | α | D_1 |
|-----|-------------|------------|-------|
| 1 | 0.641945321 | 1.49567371 | 0 |

Table 4. Mooney-Rivlin hyperelastic constants for SikaFlex 252.

| N | c_{10} | c_{01} | D_1 |
|-----|------------|-------------|-------|
| 1 | 0.24159316 | -0.05185012 | 0 |

Table 5. Relative error obtained with the different models for the SikaFlex 252 SLJ joints.

| Model | Relative error (SLJ 1mm) | Relative error (SLJ 3mm) |
|---------------|--------------------------|--------------------------|
| Ogden $N=2$ | 75 % | 18 % |
| Ogden $N=1$ | 13 % | 43 % |
| Mooney Rivlin | 2.6 % | 4.2 % |

Finally, in order to quantify the differences between the performances observed for the different material models, the relative error between the experimental curve and the one obtained with each model, has been integrated over the whole measurement range. The results are shown in Table 5.

4. Conclusions

In this study, a methodology has been defined to characterise high flexibility adhesives. After a preliminary experimental study of different adhesives, the best performing one was selected as representative for further characterisation. Uniaxial tensile and pure shear tests (planar test) were then used to characterise the material. From there, simulation was used to fit the constants of different theoretical models of hyperelastic material, in order to select those that offered the best fit. Subsequently, to validate the performance offered by these models, specimens working in shear (SLJ) were simulated, and the following conclusions were reached:

- The Ogden model of order 2, which was selected a priori as the best, has given a good correlation in SLJ tests with adhesive thicknesses of 3 mm (the same thickness used in the characterisation tests in the previous phase). However, it does not provide valid results at lower thicknesses.
- The best results have been obtained with a Mooney-Rivlin model, starting from the one that had given good results in the characterisation of the uniaxial tensile test, after a small iterative modification of the parameters.
- These results show that it is possible to obtain a single hyperelastic material behaviour law, valid to represent the behaviour of different configurations and thicknesses of highly flexible adhesive. However, in the process of selecting and fitting the material model and its constants, the validity of the adhesive material characterisation tests used in this study, and in particular the planar test as defined here, is called into question.

As future lines of research, it is proposed precisely to define the appropriate characterisation tests, specifically defined for this type of hyperelastic adhesives, which will allow a more precise adjustment of the behavioural law.

Author Contributions

F.J. Simón: Methodology, Software, Writing - Original Draft; O. Cuadrado: Validation, Resources; E.A.S. Marques: Methodology, Software; M. Sánchez: Formal analysis, Writing - Review and Editing, Methodology; L.F.M da Silva: Supervision and Methodology. All authors discussed the results, reviewed, and approved the final version of the manuscript.

Acknowledgement

Not applicable.

Conflict of Interest

The authors declared no potential conflicts of interest concerning the research, authorship, and publication of this article.

Funding

The authors received no financial support for the research, authorship, and publication of this article.

Data Availability Statements

The datasets generated and/or analyzed during the current study are available from the corresponding author on reasonable request.

References

- [1] P. J. Winkler, *Materials for transportation technology*, Wiley, p. 372, 2000.
- [2] B. Burchardt, *Advances in polyurethane structural adhesives*, in: *Adv. Struct. Adhes. Bond.*, Woodhead Publishing, pp. 35–65, 2010.



- [3] R. P. Campion, *Engineering with Rubber: How to Design Rubber Components*, Hanser, p. 434, 2001.
- [4] A. L. Loureiro, L. F. M. Da Silva, C. Sato, and M. A. V. Figueiredo, Comparison of the mechanical behaviour between stiff and flexible adhesive joints for the automotive industry, *J. Adhes.*, 86(7), 2010, 765–787.
- [5] M. D. Banea and L. F. M. Da Silva, Adhesively bonded joints in composite materials: An overview, *Proc. Inst. Mech. Eng. Pt. L J. Mat. Des. Appl.*, 223(1), 2009, 1–18.
- [6] J. Mauricea, J. Y. Cognard, R. Creac'Hcade, P. Davies, L. Sohier, and S. Mahdi, Characterization and modelling of the 3D elastic-plastic behaviour of an adhesively bonded joint under monotonic tension/compression-shear loads: Influence of three cure cycles, *J. Adhes. Sci. Technol.*, 27(2), 2013, 165–181.
- [7] I. Lubowiecka, M. Rodríguez, E. Rodríguez, and D. Martínez, Experimentation, material modelling and simulation of bonded joints with a flexible adhesive, *Int. J. Adhes. Adhes.*, 37, 2012, 56–64.
- [8] O. Hesebeck and A. Wulf, Hyperelastic constitutive modeling with exponential decay and application to a viscoelastic adhesive, *Int. J. Solids Struct.*, 141–142, 2018, 60–72.
- [9] V. Dias, C. Odenbreit, O. Hechler, F. Scholzen, and T. Ben Zineb, Development of a constitutive hyperelastic material law for numerical simulations of adhesive steel-glass connections using structural silicone, *Int. J. Adhes. Adhes.*, 48, 2014, 194–209.
- [10] R. D. S. G. Campilho, M. D. Banea, J. A. B. P. Neto, and L. F. M. Da Silva, Modelling adhesive joints with cohesive zone models: Effect of the cohesive law shape of the adhesive layer, *Int. J. Adhes. Adhes.*, 44, 2013, 48–56.
- [11] P. Boulanger and M. Hayes, *Finite-Amplitude Waves in Mooney-Rivlin and Hadamard Materials*, in *Topics in Finite Elasticity*, Springer, Vienna, 2001.
- [12] M. Sasso, G. Palmieri, G. Chiappini, and D. Amodio, Characterization of hyperelastic rubber-like materials by biaxial and uniaxial stretching tests based on optical methods, *Polym. Test.*, 27(8), 2008, 995–1004.
- [13] Y. Xia, Y. Dong, Y. Xia, and W. Li, A novel planar tension test of rubber for evaluating the prediction ability of the modified eight-chain model under moderate finite deformation, *Rubber Chem. Technol.*, 78(5), 2005, 879–892.
- [14] A. Aidy, M. Hosseini, and B. B. Sahari, A Review of Constitutive Models for Rubber-Like Materials, *Am. J. Eng. Appl. Sci.*, 3(1), 2010, 232–239.
- [15] A. K. Bazkiaei, K. H. Shirazi, and M. Shishesaz, A framework for model base hyper-elastic material simulation, *J. Rubber Res.*, 23(4), 2020, 287–299.
- [16] G. Chagnon, G. Marckmann, and E. Verron, A comparison of the Hart-Smith model with Arruda-Boyce and Gent formulations for rubber elasticity, *Rubber Chem. Technol.*, 77(4), 2004, 724–735.
- [17] R. S. Rivlin, Large elastic deformations of isotropic materials IV. further developments of the general theory, *Philos. Trans. R. Soc. London. Ser. A, Math. Phys. Sci.*, 241(835), 1948, 379–397.
- [18] M. C. Boyce and E. M. Arruda, Constitutive models of rubber elasticity: A review, *Rubber Chem. Technol.*, 73(3), 2000, 504–523.
- [19] İ. D. Külçü, A hyperelastic constitutive model for rubber-like materials, *Arch. Appl. Mech.*, 90(3), 2020, 615–622.
- [20] *Abaqus Analysis User's Manual*, Abaqus 6.12.
- [21] D. J. Charlton, J. Yang, and K. K. Teh, Review of methods to characterize rubber elastic behavior for use in finite element analysis, *Rubber Chem. Technol.*, 67(3), 1994, 481–503.
- [22] M. Mooney, A theory of large elastic deformation, *J. Appl. Phys.*, 11(9), 1940, 582–592.
- [23] O. H. Yeoh, Some forms of the strain energy function for rubber, *Rubber Chem. Technol.*, 66(5), 1993, 754–771.
- [24] R. W. Ogden, Large deformation isotropic elasticity – on the correlation of theory and experiment for incompressible rubberlike solids, *Proc. R. Soc. London. A. Math. Phys. Sci.*, 326(1567), 1972, 565–584.
- [25] L. E. Crocker, B. C. Duncan, R. G. Hughes, and J. M. Urquhart, *Hyperelastic Modelling of Flexible Adhesives*, 1999, 1–42.
- [26] B. Kim et al., A comparison among Neo-Hookean model, Mooney-Rivlin model, and Ogden model for Chloroprene rubber, *Int. J. Precis. Eng. Manuf.*, 13(5), 2012, 759–764.
- [27] ISO 37:2011 - *Rubber, vulcanized or thermoplastic — Determination of tensile stress-strain properties*, 2011.
- [28] D. Moreira, L. N.-P. Testing, *Comparison of simple and pure shear for an incompressible isotropic hyperelastic material under large deformation*, Elsevier, 2013.
- [29] M. Shahzad, A. Kamran, M. Z. Siddiqui, and M. Farhan, Mechanical characterization and FE modelling of a hyperelastic material, *Mater. Res.*, 18(5), 2015, 918–924.
- [30] ASTM D1002-01., Standard Test Method for Apparent Shear Strength of Single-Lap-Joint Adhesively Bonded Metal Specimens by Tension Loading (Metal-to-Metal).
- [31] UNE EN ISO 9664:1996 ADHESIVES. TEST METHODS FOR FATIGUE PROPERTIES OF STRUCTURAL ADHESIVES IN TENSILE SHEAR.

ORCID iD

Francisco J. Simon Portillo  <https://orcid.org/0000-0003-1954-6743>

Óscar Cuadrado Sempere  <https://orcid.org/0000-0002-4376-5033>

Eduardo A.S. Marques  <https://orcid.org/0000-0002-2750-8184>

Miguel Sánchez Lozano  <https://orcid.org/0000-0002-7520-8522>

Lucas F.M. da Silva  <https://orcid.org/0000-0003-3272-4591>



© 2022 Shahid Chamran University of Ahvaz, Ahvaz, Iran. This article is an open access article distributed under the terms and conditions of the Creative Commons Attribution-NonCommercial 4.0 International (CC BY-NC 4.0 license) (<http://creativecommons.org/licenses/by-nc/4.0/>).

How to cite this article: Simon Portillo F.J., Cuadrado Sempere Ó., Marques E., Sánchez Lozano M., da Silva L.F.M. Mechanical Characterization and Comparison of Hyperelastic Adhesives: Modelling and Experimental Validation, *J. Appl. Comput. Mech.*, 8(1), 2022, 359–369. <https://doi.org/10.22055/JACM.2021.38119.3242>

Publisher's Note Shahid Chamran University of Ahvaz remains neutral with regard to jurisdictional claims in published maps and institutional affiliations.

